J Mater Sci (2007) 42:9827–9835
DOI 10.1007/s10853-007-2008-9

The structure and properties of silver-doped phosphate-based glasses

**I. Ahmed · E. A. Abou Neel · S. P. Valappil ·
S. N. Nazhat · D. M. Pickup · D. Carta · D. L. Carroll ·
R. J. Newport · M. E. Smith · J. C. Knowles**

Received: 5 February 2007 / Accepted: 20 July 2007 / Published online: 21 August 2007

Abstract An undoped and two silver-doped (0, 3 and 5 mol% Ag) phosphate glass compositions were investigated for their structure and properties. These compositions had in a previous study been investigated for their antimicrobial properties, and were found to be extremely potent at inhibiting the micro-organisms tested. Thermal, X-ray diffraction (XRD), nuclear magnetic resonance (NMR) and X-ray absorption Near Edge Structure (XANES) studies were used to elucidate the structure of the compositions investigated, whilst degradation and ion release studies were conducted to investigate their properties. No significant differences were found between the T_g values of the silver containing glasses, while XRD analysis revealed the presence of a $NaCa(PO_3)_3$ phase. NMR showed the dominance of Q^2 species, and XANES studies revealed the oxidation state of silver to be in the +1 form. No correlation was seen between the degradation and cation release profiles observed, and the $P_3O_9^{3-}$ anion was the highest released anionic species, which correlated well with the XRD and NMR studies. Overall, it was ascertained that using Ag_2SO_4 as a precursor, and producing compositions containing 3 and 5 mol% Ag, the levels of silver ions released were within the acceptable cyto/biocompatible range.

Introduction

Glasses in the P_2O_5–CaO–Na_2O system have a chemical composition similar to that of the inorganic phase of bone. These glasses consist of PO_4 tetrahedra, which can be attached to a maximum of three neighbouring tetrahedra forming a three dimensional network as in vitreous P_2O_5 [1]. Adding metal oxides to the glass leads to a depolymerisation of the network, with the breaking of P–O–P linkages and the creation of non-bridging oxygens. The modifying cations can provide ionic cross-linking between the non-bridging oxygens of two phosphate chains, thus increasing the bond strength of this ionic cross-link and improving the mechanical strength and chemical durability of the glasses [2].

These phosphate-based glasses (PBG) are a unique class of materials in that they are completely degradable; whereas silica-based glasses are relatively stable to hydrolysis. Furthermore, the degradation of PBG can be tailored to suit the end application [3], and the rate at which they hydrolyse can vary quite considerably. For example, binary sodium phosphate glass compositions can dissolve within a few hours in dH_2O, whereas high iron oxide containing glasses have been known to exhibit dissolution rates even lower than that of commercially produced glass

I. Ahmed · E. A. Abou Neel · S. P. Valappil ·
S. N. Nazhat · J. C. Knowles (✉)
Division of Biomaterials and Tissue Engineering, Eastman
Dental Institute, University College London, 256 Gray's Inn
Road, London WC1X 8LD, UK
e-mail: j.knowles@eastman.ucl.ac.uk

S. N. Nazhat
Department of Mining, Metals, and Materials Engineering,
McGill University, 3610 University Street Montreal, H3A 2B2
QC, Canada

D. M. Pickup · D. Carta · R. J. Newport
School of Physical Sciences, University of Kent, Canterbury
CT2 7NH, UK

D. L. Carroll · M. E. Smith
Department of Physics, University of Warwick, Coventry
CV4 7AL, UK

for windows, and have also been investigated to be used in the immobilisation of nuclear waste materials [4].

Controlled release glasses (CRG) developed during the last two decades are based on phosphates of calcium and sodium. They can be produced in many physical forms, such as powder granules, fibres, cast blocks of various shapes or as tubes [5]. Gilchrist et al. [5] and Lenihan et al. [6] both investigated CRG-based tubes for the repair of peripheral nerve injuries. Their findings were consistent with the view that regeneration of the nerves had taken place to a degree at least as effective as that seen in nerves of similar size repaired by conventional means. Lenihan et al. also suggested that the ends of the nerves could be secured in the tube with fibrin glue; thus, the CRG could prove to be beneficial in situations where microsurgical facilities were not available.

Examples of CRGs have also found application in the controlled supply of Cu, Co and Zn to cattle, and it was ascertained that no ill effects were observed [7] after having fed these glasses to the animals to tackle trace element deficiencies. Applications ranging from orthodontic devices to nutritional experiments with rats (with the CRG pellets being implanted subcutaneously, intramuscularly and intraperitoneally in the rats) [5, 8] have also been investigated.

Recently, Avent et al. [9] investigated a CRG incorporating silver for the delivery of a constant concentration of silver ions in aqueous flow systems for the control of urinary tract infections. It was found that the concentration of silver ions released from the glasses was dependant on the glass composition. The glasses investigated by Avent et al. contained high sodium oxide and low calcium oxide concentrations; thus, these glasses would have been relatively highly soluble.

The PBG investigated in this study have a fixed phosphate content of 50 mol%, and a fixed CaO content of 30 mol%. The remainder is made up from Na_2O, with substitution for Ag ions at 3 and 5 mol% (the silver was incorporated as Ag mol%, as the final oxidation state of the silver was being investigated, and is one of the themes of this investigation). These compositions have recently been evaluated for their antibacterial and antimicrobial activity against *Staphylococcus aureus*, *Escherichia coli*, *Bacillus cereus, Pseudomonas aeruginosa*, methicillin-resistant *Staphylococcus aureus* (MRSA) and *Candida albicans* [10]. It was found that incorporation of 3 mol% Ag was more than sufficient to mount a potent and long term antimicrobial effect against these organisms. Also from the degradation studies conducted in the Nutrient Broth [10], which was used for the associated microbiological assays, a decrease in the degradation rates was observed, and it was suggested that this may been have been due to Ag present in its +2 oxidation state, thus cross-linking the phosphate chains, along with the Ca^{2+} ions. Therefore, the main purpose of this present study was to elucidate the oxidation state of the silver present within the glass, and to also investigate the structure and properties of these silver-doped PBG using thermal analysis, X-ray diffraction (XRD), degradation, ion release, nuclear magnetic resonance (NMR) and X-ray absorption Near Edge Structure (XANES) studies.

Materials and methods

Glass preparation

Glass compositions were prepared using NaH_2PO_4, $CaCO_3$, P_2O_5 (BDH, UK) and Ag_2SO_4 (Sigma Aldrich, UK) as starting materials. The precursors were weighed out and placed into a 200 mL silica crucible (Saint-Gobain, UK). The crucible was placed into a furnace, and the glass was melted at 1,100 °C for 1 h. The molten glass was then poured into a 5 mm diameter graphite mould, which had been preheated to 370 °C. The mould was then left to slowly cool to room temperature in order to remove any residual stress. Glass rods obtained from the mould were cut into 2 mm thick discs using a Testbourne diamond saw with methanol as the cutting/lubrication agent. See Table 1 for glass codes of compositions investigated.

Thermal analysis

Pieces of glass of the varying compositions were ground using a vibratory agate mill. Three main thermal parameters were measured; the glass transition temperature, T_g, the crystallisation temperature, T_c, and the melting

Table 1 Glass codes and compositions investigated in this study, with their corresponding degradation rates obtained

Glass codes	Composition in mol%				Dissolution rates (mg mm^{-2} h^{-1})/R^2 value
	P_2O_5	CaO	Na_2O	Ag	
0 mol% Ag	50	30	20	0	0.0015/0.899
3 mol% Ag	50	30	17	3	0.0014/0.848
5 mol% Ag	50	30	15	5	0.0009/0.835

temperature, T_m. The analysis was conducted on a Setaram differential thermal analyser (DTA), using an inert nitrogen atmosphere at a heating rate of 20 °C min^{-1} up to a maximum of 1,000 °C. The data was baseline-corrected by carrying out a blank run and subtracting this from the original plot.

XRD analysis

The glass discs were annealed at their respective crystallisation temperatures (obtained from thermal analyses) for 2 h to investigate the phases that crystallised from the glass. The data was collected on a Brüker D8 Advance diffractometer in flat plate geometry, using Ni filtered Cu K_α radiation. Data was collected from 10° to 100° in 2θ, with a step size of 0.02° and a count time of 12 s per point. The phases were identified with Crystallographica Search-Match Software (Oxford Cryosystems, Oxford, UK) and the ICDD database (vols 1–42)

NMR analysis

The ^{31}P MAS NMR spectra were accumulated on a Varian-Chemagnetics CMX Infinity spectrometer equipped with an 8.45 T magnet using a 4 mm probe with the sample spinning at $\sim$12 kHz. The spectra were accumulated at a frequency of 145.85 MHz with a single pulse of 2 μs (corresponding to a tip angle of 90°) and a recycle delay of 3 s. The spectra were referenced against a secondary reference of $NH_4H_2PO_4$ at a shift of 0.9 ppm such that the spectrum is reported on a shift scale relative to the primary shift reference of 85% H_3PO_4.

XANES study

Ag K-edge XANES measurements were made at a temperature of approximately 77 K on Station 16.5 at the Synchrotron Radiaton Source (SRS, Daresbury Laboratory, UK) with a synchrotron ring energy of 2 GeV and a stored current of 150–250 mA. The spectra were recorded in transmission mode using a double crystal Si (220) monochromator (d = 1.92 Å) and ionisation chambers to detect the incident and transmitted beam intensities, I_i and I_t respectively. Finely-ground samples were diluted in polyethylene (Aldrich, spectrophotometric grade) and pressed into pellets to give a satisfactory K-edge absorption step. A silver foil and a third ionisation chamber were placed after the sample's transmission ionisation chamber to allow an absorption spectrum of the foil to be collected simultaneously for the purpose of calibration of the energy scale which was defined by assigning the maximum of the derivative of the Ag foil spectrum to 25521.0 eV.

XANES spectra were collected from 200 eV below to 250 eV above the Ag K-edge in order to allow accurate background subtraction. A fine energy step of 0.3 eV was used around the edge; this being significantly smaller than the intrinsic width of the Ag K-edge induced by core-hole lifetime broadening effects. The data processing comprised conversion of the data to absorption versus energy, calibration of the energy scale, removal of the pre-edge absorption by straight-line fitting to $\mathrm{Log}(I_\mathrm{i}/I_0)$, and removal of the post-edge atomic absorption profile by fitting with a second order polynomial. All the spectra were normalised to have an edge-step of unity. Spectra were also collected from a series of reference materials: AgO (Aldrich), Ag_2O (99.99+%, Aldrich), Ag_2SO_4 ($\geq$99.99%, Aldrich) and Ag_3PO_4 (98%, Aldrich).

Degradation studies

The surface area of the glass discs was calculated from the dimensions obtained via a pair of vernier callipers prior to placing them in containers. Twenty five millilitres of pH-adjusted (pH 7 ± 0.2) deionised water was added to these containers, and the discs (approximately 5 × 2 mm) were placed into them, which were then incubated at 37 °C, and agitated at 200 revolutions per minute (rpm). At various time points (2, 4, 6 and then every 24 h), the discs were taken out of their respective containers, and excess moisture was removed by blotting the samples dry with tissue. After having weighed the disks, they were then placed into a fresh solution of deionised water, and were then placed back into the 37 °C incubator, and agitated at 200 rpm. The experiments were conducted for up to 120 h. As the dissolution rate of the discs is affected by surface area, the data was presented as weight loss per unit area. To obtain the rate of weight loss, the initial mass (M_0) of each sample was measured as well as mass at time t (M_t) to give a weight loss per unit area thus:

Weight loss = $(M_0-M_t)/A$, where A is the surface area (mm^2). The measurements were carried out in triplicate. The data was plotted as weight loss per unit area against time. These glasses are know to have two distinct dissolution events depending on composition, an early stage event with a $t^{1/2}$ relationshiop and a later linear relationship. Fitting of the data through the complete data set or a partial set after the initial event gave the same slope values, but with differing R^2 values. The slope values presented are for curves fitted through data from 24 h onwards. The slope of this graph gave a dissolution rate value in terms of mg $\mathrm{mm}^{-2}\ \mathrm{h}^{-1}$, which was determined by fitting a straight line through the data and also passing through the origin. The dissolution plots obtained were linear. (See Table 1 for dissolution rates obtained).

pH Measurements

pH measurements of the solution were taken at every time point, after having transferred the glass discs to a fresh solution. The measurements were collected using a Hanna Instruments pH 211 Microprocessor pH meter (BDH, UK) with attached glass combination pH electrode (BDH, UK). The pH electrode was calibrated using pH calibration standards (Colourkey Buffer Solutions. BDH, UK).

Ion release studies

The solutions obtained at each time point from the degradation studies were analysed for sodium, calcium, phosphate and silver ion release.

Cation release studies

For the cation release studies, an ICS-1000 ion chromatography system (Dionex, UK) was used. A 30 mM MSA (Methanesulfonic acid, BDH, UK) solution was used as the eluent. The ICS-1000 is an integrated and preconfigured system that performs isocratic IC separations using suppressed conductivity detection. In this method, cations were eluted using a 4 × 250 mm IonPac® CS12A separator column. All results were calculated against a 4-point calibration curve using the predefined calibration routine. Coupled with AutoSuppression®, the ICS-1000 provides high performance with ease of use. Chromeleon® software package was used for data analysis.

Cation reagent and standard solution preparation

Sodium chloride (Sigma, UK) and calcium chloride ($CaCl_2.2H_2O$) (BDH, UK) were used as reagents. A 100 ppm mixed (sodium and calcium) stock solution was prepared, from which serially diluted 50, 25, 10 and 1 ppm standard solutions were obtained.

Anion release studies

The phosphate anion measurements were conducted on a Dionex ICS-2500 ion chromatography system (Dionex, UK), consisting of a gradient pump with a 25-μl sample loop. The anions were eluted using a 4 × 250 mm IonPac® AS16 anion-exchange column packed with anion exchange resin. A Dionex ASRS® (Anion Self-Regenerating Suppressor) was used at 223 mA. The Dionex EG40 eluent generator equipped with a potassium hydroxide cartridge was used in conjunction with the ASRS®. The EG40 eluent generator system electrolytically produces high-purity KOH eluents using deionised water as the carrier stream at the point of use. The use of the EG40 hydroxide eluent generator leads to negligible baseline shifts during the hydroxide gradients, along with greater retention time reproducibility. The sample run time was set for 20 min. The gradient program started from 30 mM KOH, and after 5 min increased to 60 mM KOH over a 10 min duration, and then maintained at 60 mM KOH for a further 3 min. This concentration then declined back to 30 mM over a 1 min period, and stayed at 30 mM for a further minute. The Chromeleon® software package was used for data analysis.

Anion reagents and standard solution preparation

Tribasic sodium phosphate (Na_3PO_4), trisodium trimetaphosphate ($Na_3P_3O_9$), pentasodium tripolyphosphate ($Na_5P_3O_{10}$), (Sigma, UK) and tetra-sodium pyrophosphate ($Na_4P_2O_7$) (BDH, UK) were used as reagents. A 100 ppm working solution containing all of the above 4 reagents was prepared, from which serially diluted 50, 25, 10 and 1 ppm standard solutions were obtained. Higher phosphate group containing reagents (i.e., P_4 or above) were not commercially available.

Silver ion release

Silver ion release was measured using the commercially available silver test kit (Silver Test Kit 1.14831.0001, Merck, UK). The test worked on the principle that in a weakly acidic solution, silver ions react with phenanthroline and eosine to form a red complex, the concentration of which is determined photometrically (at 552 nm). A silver standard solution, 1,000 mg/L Ag, provided by the supplier, was used to prepare the calibration curve. In the event of silver concentrations exceeding 5 mg/L, samples were diluted before measurement. For all samples tested, high purity water was used to make the blank.

Results

Thermal analysis

As can be seen from Fig. 1, there was an increase in T_g by incorporating Ag in the glass composition at 3 mol%.

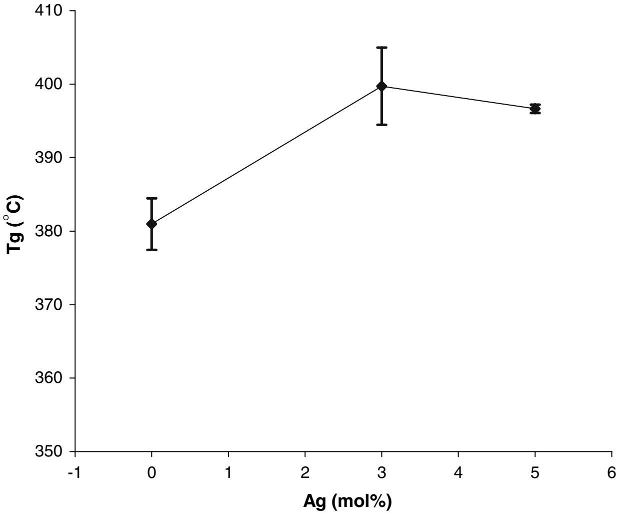

Fig. 1 T_g values obtained of silver-doped phosphate-based glasses with 0, 3 and 5 mol% Ag

However, there was no significant difference in T_g of glasses containing 3 and 5 mol% Ag. Other Ag-doped compositions (containing 1 to 5 and 10 and 20 mol% Ag) were also analysed for their thermal properties; however, no discernible patterns or profiles could be observed. The data obtained for T_c and T_m also showed no pattern in the profiles observed either.

XRD analysis

The XRD analysis demonstrated that the same phase was identified for all three compositions investigated. This was the $NaCa(PO_3)_3$ phase, a sodium calcium metaphosphate (see Table 2). Some peaks could not be matched, and this suggested the possibility of another phase present (indicated in Table 2 with a *); however, these were too few to allow for any accurate assignment to be made.

NMR analysis

In the ^{31}P MAS NMR spectra for both the 0 and 5 mol% silver-doped glasses, a single isotropic peak at −26 ppm is observed with a series of accompanying spinning sidebands. This peak shift corresponds to a Q^2 species [11], meaning that each phosphorus atom is linked with two bridging oxygen atoms per phosphate tetrahedron (see Fig. 2).

Table 2 Phases identified from XRD analysis, using Crystallographic Software, and the ICDD database (vols 1–42), with their corresponding phase card numbers

Composition	XRPD Phases	
	Phase 1	Phase 2
0 mol% Ag	$NaCa(PO_3)_3$/23–669	*
3 mol% Ag	$NaCa(PO_3)_3$/23–669	*
5 mol% Ag	$NaCa(PO_3)_3$/23–669	

XANES analysis

The Ag K-edge XANES spectra from the reference compounds are shown in Fig. 3. The position of the X-ray absorption edge in each spectrum contains information on the oxidation state of the silver ions present. As expected, the edge position of AgO, which contains a mixture of Ag^I and Ag^{III} ions [12], appears at the highest energy since it requires more energy to remove electrons from the higher valence ions. The absorption edges of the Ag^I compounds all appear at lower energy. The apparent shift in edge

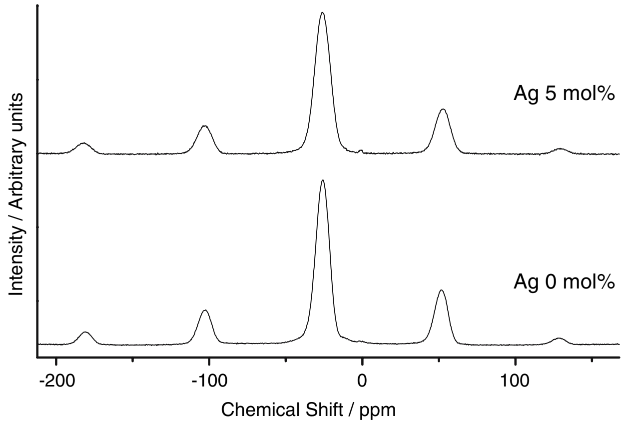

Fig. 2 ^{31}P MAS NMR spectra of glasses with 0 mol% and 5 mol% Ag

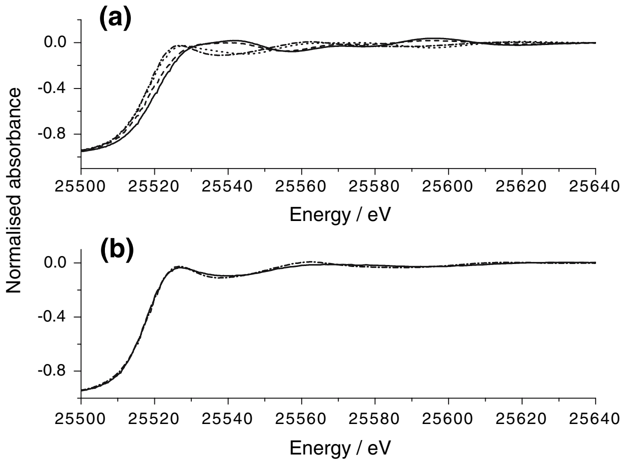

Fig. 3 Ag K-edge XANES spectra. (**a**) reference compounds: AgO (–), Ag_2O (- - -), Ag_3PO_4 (···) and Ag_2SO_4 (–·–) and (**b**) 5 mol% Ag glass (–) compared with Ag_2SO_4 (–·–)

position between Ag_2O and the remaining two Ag^I compounds is due to the greater width of the absorption edge in the former and is a result of the differing structural environments of the silver ions. In general, the Ag K-edge becomes sharper as the number of oxygen atoms surrounding the silver ions increases [12]. In Ag_2O, the silver ions are coordinated to two oxygen atoms whereas in Ag_2SO_4 and Ag_3PO_4 the Ag–O coordination numbers are six and eight, respectively [13]. The spectrum from the 5 mol% Ag glass plotted in Fig 3b, is very similar to that from Ag_2SO_4 (also plotted).

Degradation analysis

As can be seen from the dissolution data (Fig. 4), there were no perceptible differences in the profiles of the 0 and 3 mol% Ag compositions. The profile of the 5 mol% Ag composition did however exhibit a reduced degradation rate. The dissolution rates obtained by applying a line of best fit through the data for the 0, 3 and 5 mol% Ag compositions were 0.0015, 0.0014 and 0.0009 mg mm^2 h^{-1}, respectively.

pH analysis

The pH analysis revealed that the 0 mol% composition remained relatively neutral for the duration of the study. However, the pH dropped to around 5.5 for the 3 and 5 mol% Ag compositions. The profiles observed for the 3 and 5 mol% Ag compositions were almost identical (see Fig. 5).

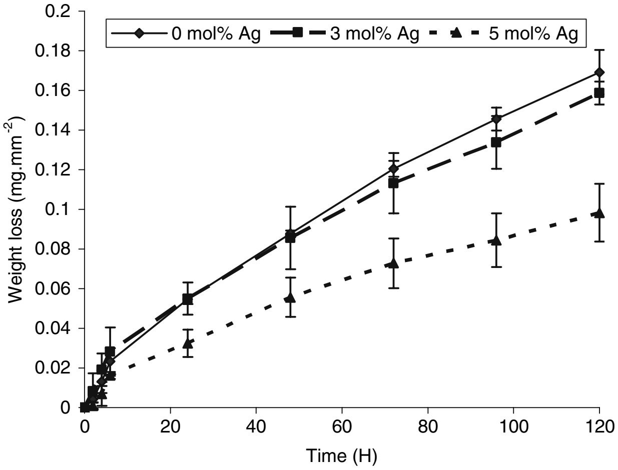

Fig. 4 Degradation profiles obtained from cumulative studies conducted in dH_2O, for glass with 0, 3 and 5 mol% Ag. (Lines added to show profiles)

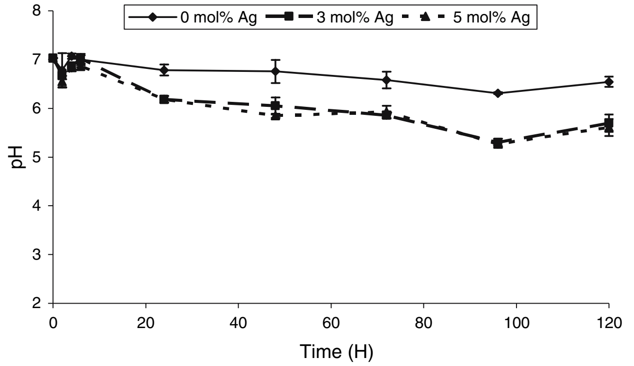

Fig. 5 pH profiles obtained from cumulative studies conducted in dH_2O for glasses with 0, 3 and 5 mol% Ag. (Lines added to show profiles)

Ion release studies

Cation analyses

It was seen from Fig. 6a–b that equal amounts of sodium and calcium ions were released from the compositions investigated. The sodium ion release profiles showed clear

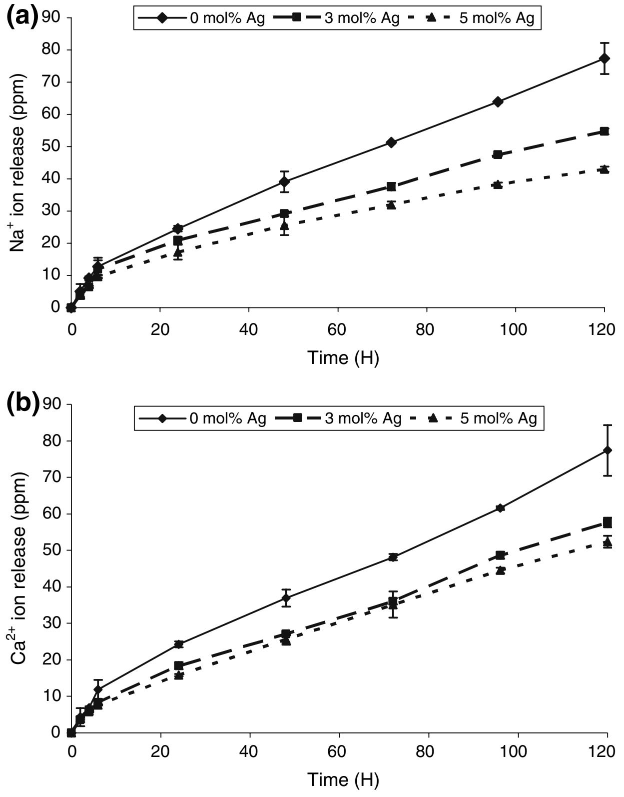

Fig. 6 (**a**) Sodium ion release profiles obtained from cumulative studies in dH_2O for silver-doped PBG with 0, 3 and 5 mol% Ag. (**b**) Calcium ion release profiles obtained from cumulative studies in dH_2O for silver-doped PBG with 0, 3 and 5 mol% Ag

differences between the compositions investigated, with a decrease in Na^+ ion release seen with increasing Ag mol%. The highest sodium ion release was seen for the 0 mol% Ag composition, which was expected as the Ag ions were added in place of Na_2O, therefore, there was less sodium present in the other two compositions.

For the calcium ion release profiles (Fig. 6b), again the 0 mol% Ag composition released the highest amount of ions, with little difference seen between the 3 mol% and 5 mol% Ag compositions.

Anion analyses

As seen from Fig. 7a, only small amounts of the PO_4^{3-} anion were released between each time point. The profiles appear to be linear in nature, and no difference was observed between the three compositions investigated.

For the $P_2O_7^{4-}$ anion release (Fig. 7b), again there was no difference seen between the compositions investigated, as this anion was released in very small quantities.

The $P_3O_9^{3-}$ anion was the one released at the greatest rate out of the four anions investigated (see Fig. 7c). The 0 mol% Ag composition released the highest levels of this anion, with the 3 and 5 mol% Ag compositions exhibiting no differences between them. The release profile of this anionic species mirrored that of the calcium ion release.

Just as was the case for the $P_2O_7^{4-}$ anion, the $P_3O_{10}^{5-}$ anion was also released at very low levels as shown in Fig. 7. The 0 mol% Ag composition released the highest amount, with no differences again seen between the 3 mol% and 5 mol% Ag compositions.

Ag ion release

As can be seen from Fig. 8, no silver was detected from the 0 mol% Ag composition as expected, however clear differences are seen between the 3 mol% Ag and 5 mol% Ag compositions, with the 5 mol% Ag composition releasing the highest amount of Ag ions.

Discussion

The purpose of this study was to investigate the structure and properties of PBG doped with 3 and 5 mol% Ag. These compositions were recently [10] investigated for their antimicrobial effect on various organisms. Silver was calculated and added as mol% of Ag instead of silver oxide (either Ag_2O or AgO), due to the final oxidation state of silver being unknown after having melted the glass at 1,100 °C. Therefore, elucidating the oxidation state of silver with regards to the precursor used was also one of the remits of this paper.

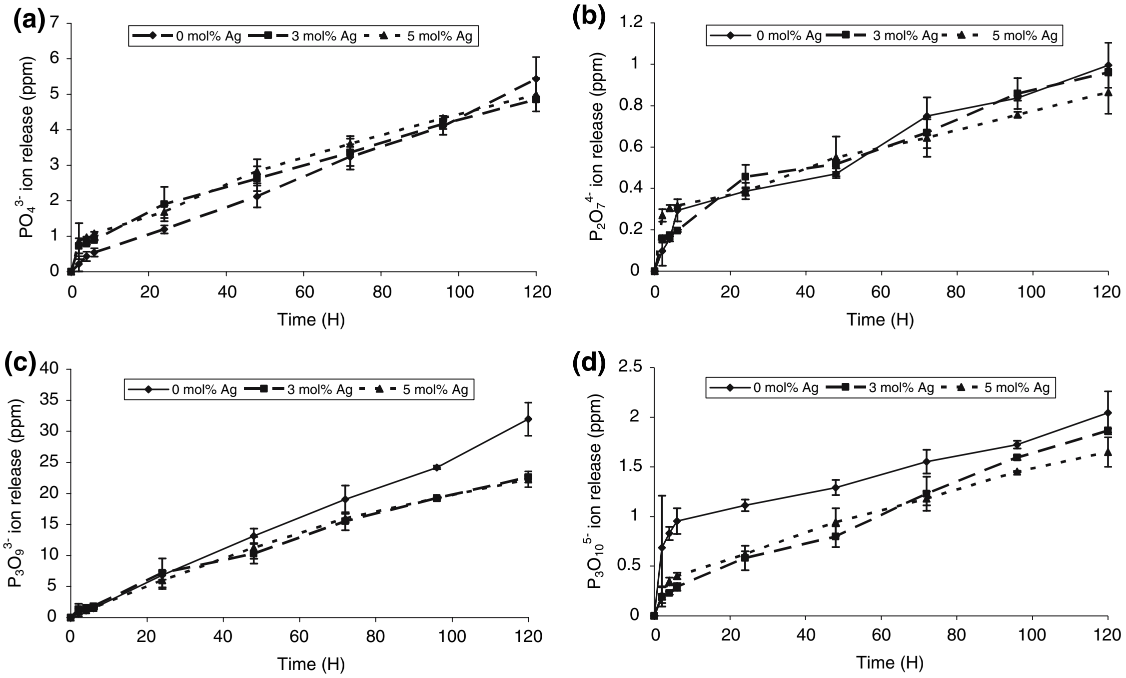

Fig. 7 (**a**) PO_4^{3-} anion release profiles obtained from cumulative studies in dH_2O for silver-doped PBG with 0, 3 and 5 mol% Ag. (**b**) $P_2O_7^{4-}$ anion release profiles obtained from cumulative studies in dH_2O for silver-doped PBG with 0, 3 and 5 mol% Ag. (**c**) $P_3O_9^{3-}$ anion profiles obtained from cumulative studies in dH_2O for silver-doped PBG with 0, 3 and 5 mol% Ag. (**d**) $P_3O_{10}^{5-}$ anion release profiles obtained from cumulative studies in dH_2O for silver-doped PBG with 0, 3 and 5 mol% Ag

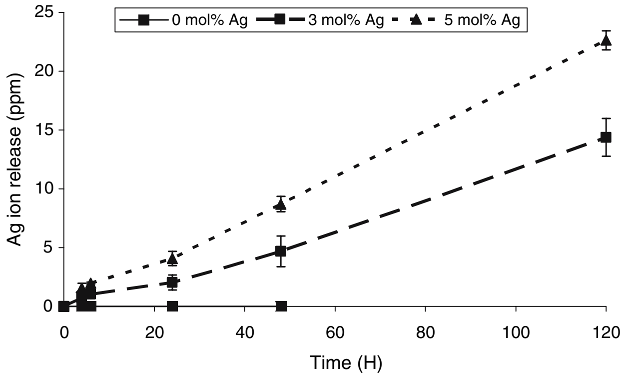

Fig. 8 Ag^+ ion release profiles obtained from cumulative studies in dH_2O for silver-doped PBG with 0, 3 and 5 mol% Ag

From the thermal analyses conducted, no pattern was observed with the doped samples with increasing Ag mol%. It was seen from the XRD data obtained that only the $NaCa(PO_3)_3$ crystalline phase was identified for all three compositions investigated after annealing the compositions at T_c. This phase has also been previously identified for crystallised (devitrified) glass compositions containing a fixed phosphate content of 50 mol% [2, 14].

NMR studies revealed that a Q^2 species dominated the structure of the glasses investigated. From models proposed for phosphate glasses, this agreed accurately with the predicted model for metaphosphate glasses (i.e., 50 mol% P_2O_5) where the network should be based exclusively on Q^2 tetrahedra, forming chains and/or rings [2, 11, 15]. The data here clearly shows that the phosphate network was unaltered by exchanging sodium with silver for up to one quarter of the initial sodium content. This also correlated well with the XRD studies where the crystalline phase identified after annealing the glass at T_c was a cyclic Q^2 species (namely, P_3O_9).

XANES studies were undertaken to elucidate the oxidation state of silver in the compositions investigated. The Ag K-edge XANES spectra from the reference compounds are shown in Fig. 3a. Comparing the XANES spectrum from the 5 mol% Ag glass sample with that from Ag_2SO_4 in Fig. 3b, it can be seen that the position of the X-ray absorption edges are the same. Since Ag_2SO_4 contains Ag^I ions, it can be concluded from this result that the phosphate glass compositions investigated also contain silver in the monovalent oxidation state. Furthermore, the shape of the spectra from the phosphate glass and Ag_2SO_4 are very similar suggesting that the structural environment of the Ag^I ions is similar in both cases. Since Ag_2SO_4 contains silver ions surrounded by a distorted octahedron of oxygen atoms [13], it follows that the silver ions in the phosphate glasses investigated most probably reside in such an environment. This structural assignment remains tentative, however, due to the relative insensitivity of Ag K-edge XANES spectra to more subtle changes in the coordination sphere of oxygen atoms around the silver ions [16, 17]. It must be noted that silver nitrate was also investigated as a precursor to introduce silver ions into the glasses, along with Ag_2O and AgO oxides. However, these routes did not produce homogeneous transparent glasses; instead large brown streaks were observed, which suggested reduction of the silver ions. Using silver sulphate (Ag_2SO_4), however, clear transparent glasses were produced.

The glass degradation profiles showed no difference between the 0 mol% and 3 mol% Ag compositions, whilst a marked decrease in degradation was seen for the 5 mol% Ag composition. However, it must be noted that these profiles were in clear contrast to degradation profiles seen between the glasses when degradation studies of these same compositions were conducted in Nutrient Broth [10].

From the pH profiles obtained, it appears that the 3 and 5 mol% Ag compositions degraded faster, as their pH profiles dropped to slightly below 6, as compared to the 0 mol% Ag glass. The sodium and calcium ion release profiles were similar; however, the levels of release from these ions didn't show any correlation with the degradation profiles seen.

There were no differences seen between the compositions from the PO_4^{3-}, $P_2O_7^{4-}$ and $P_3O_{10}^{5-}$ release profiles. These anionic species were released in relatively tiny quantities, which was probably due to the small size of the disks used in this study, as compared with disks used in other studies [18]. The $P_3O_9^{3-}$ anion was the highest released anion; P_3O_9 (cyclic metaphosphate) was also the dominant crystalline phase identified from XRD analyses, and this has also been seen from other studies conducted [19]. Surprisingly, the release profiles for this anion matched the profile seen for the calcium ion release. This was not expected, as the cyclic $P_3O_9^{3-}$ species is usually considered not to be cross-linked, and is thought to make up the majority of the phosphate backbone.

In the previous study conducted [10] it was stated that striking a balance between antimicrobial and cyto/biocompatibility was of major importance. In order for the properties reported here to be exploited in Biomaterial/Tissue Engineering applications, the concentration of silver ions released must be kept within strictly defined limits. It has been reported by Saravanapavan et al. [20] that the minimum bactericidal concentration of silver is 0.1 ppm, and the cytotoxic concentration is 1.6 ppm for human cells. From the degradation studies conducted in this study and from the amounts of silver incorporated, it was predicted that the silver ion release should approximately be 0.1 ppm h^{-1}. The actual amounts quantified from the profiles observed in Fig. 8, were 0.1159 ppm h^{-1} for the 3 mol% Ag composition, and 0.1875 ppm h^{-1} for the 5 mol% Ag composition. Both within the limits specified above. However, it must be noted that it was unclear if the levels of 0.1 ppm and 1.6 ppm stated by Saravanapavan et al. [20], were total values, or whether they were rates in hours or days etc.

The literature shows that silver in its +1 form (oxidation state) is highly effective against bacterial microorganisms [21–23]. It has been shown in this study that using silver sulphate as a precursor; the silver remained in its +1 form even after having melted the PBG to 1,100 °C. As stated earlier, PBG are a unique class of materials, as their degradation can easily be altered to suit the end application, and these glasses can be used to release silver ions at inhibitory concentrations, over a long period of time.

Conclusions

The purpose of this study was to elucidate the structure and properties of the 0, 3 and 5 mol% Ag phosphate compositions investigated. From the thermal analyses conducted, no significant differences in the T_g of the silver containing glasses were observed. XRD data revealed the presence of a $NaCa(PO_3)_3$ phase, and NMR studies showed no shift in peaks, and identified the Q^2 species as dominant, which correlated well with the XRD data. XANES studies showed the oxidation state of the silver to be +1, and the silver environment to be similar to that in Ag_2SO_4.

From the degradation profiles observed, no differences were seen between the 0 mol% and 3 mol% Ag compositions, with a marked decrease in the 5 mol% Ag glass. The pH profiles showed a decrease in pH for the 3 and 5 mol% compositions, to just below pH 6. The Na^+ and Ca^{2+} ion release rates were similar, and no correlation with the degradation profiles was observed. Anionic release studies showed that $P_3O_9^{3-}$ was the highest released anion, which correlated well with both the XRD and NMR studies. Overall, it was ascertained that using Ag_2SO_4 as a precursor, and producing compositions with 3 and 5 mol% Ag, the levels of release for silver (+1) ions were within the acceptable cyto/biocompatible range.

Acknowledgements EPSRC is thanked for funding the UCL-Kent-Warwick collaboration on phosphate biomaterials through grants GR/T21080, EP/C000714 and EP/C000633. M.E. Smith also thanks EPSRC and the University of Warwick for partial funding of the NMR infrastructure.

References

1. Clement J, Manero JM, Planell JA, Avila G, Martinez S (1999) J Mater Sci: Mater Med 10:729
2. Ahmed I, Lewis MP, Olsen I, Knowles JC (2004) Biomaterials 25(3):491
3. Franks K, Abrahams I, Georgiou G, Knowles JC (2001) Biomaterials 22:497
4. Yu X, Day DE, Long GJ, Brow RK (1997) J Non-Cryst Solids 215:21
5. Gilchrist T, Glasby MA, Healy DM, Kelly G, Lenihan DV, McDowall KL et al (1998) Br J Plastic Surg 51:231
6. Lenihan DV, Carter AJ, Gilchrist T, Healy DM, Miller IA, Myles LM et al (1998) J Hand Surg (British and European Volume) 23B(5):588
7. Drake CF, Allen WM (1985) Biochem Soc Trans 13:516
8. Burnie J, Gilchrist T (1981) Biomaterials 2(10):244
9. Avent AG, Carpenter CN, Smith JD, Healy DM, Gilchrist T (2003) J Non-Cryst Solids 328:31
10. Ahmed I, Ready D, Wilson M, Knowles JC (2006) J Biomed Mater Res 79A:618
11. Brow RK (2000) J Non-Cryst Solids 263&264:1
12. McKeown DA, Gan H, Pegg LL (2005) J Non-Cryst Solids 351:3826
13. Fletcher DA, McMeeking RF, Parkin D (1996) J Chem Inf Comput Sci 36:746
14. Ahmed I, Collins CA, Lewis MP, Olsen I, Knowles JC (2004) Biomaterials 25(16):3223
15. Brow RK, Kirkpatrick RJ, Turner GL (1990) J Non-Cryst Solids 116:39
16. Sipr O, Dalba G, Rocca F (2004) Phys Rev B 69:134201
17. MacKenzie KJD, Smith ME (2002) Multinuclear solid-state NMR of inorganic materials. Pergamon Press, Oxford
18. Ahmed I, Lewis MP, Nazhat SN, Knowles JC (2005) J Biomater Appl 20[July]:65
19. Ahmed I, Lewis MP, Knowles JC (2005) Phys Chem Glasses 46(6):547
20. Saravanapavan P, Gough JE, Jones JR, Hench LL (2004) Key Eng Mater 254–256:1087
21. Feng QL, Wu J, Chen GQ, Cui FZ, Kim TN, Kim JO (2000) J Biomed Mater Res 52:662
22. Bellantone M, Williams HD, Hench LL (2002) Antimicrob Agents Chemother 46(6):1940
23. Kim TN, Feng QL, Kim JO, Wu J, Wang H, Chen GC et al (1998) J Mater Sci: Mater Med 9:129